Journal of Alloys and Compounds 660 (2016) 32–38

Contents lists available at ScienceDirect

Journal of Alloys and Compounds

journal homepage: http://www.elsevier.com/locate/jalcom

$LiMoO_3(IO_3)$, a novel molybdenyl iodate with strong second-order optical nonlinearity

A.H. Reshak [a], [b], [*], S. Auluck [c], [d]

[a] New Technologies – Research Centre, University of West Bohemia, Univerzitni 8, 306 14 Pilsen, Czech Republic
[b] Center of Excellence Geopolymer and Green Technology, School of Material Engineering, University Malaysia Perlis, 01007 Kangar, Perlis, Malaysia
[c] Council of Scientific and Industrial Research – National Physical Laboratory, Dr. K S Krishnan Marg, New Delhi 110012, India
[d] Department of Physics, Indian Institute of Technology, Hauz Khas, New Delhi 110016, India

ARTICLE INFO

Article history:
Received 30 August 2015
Received in revised form
22 October 2015
Accepted 11 November 2015
Available online 18 November 2015

Keywords:
Linear
Nonlinear
Second harmonic generation
Hyperpolarizability
Molybdenyl iodate

ABSTRACT

The linear and nonlinear optical susceptibilities of molybdenyl iodate $LiMoO_3(IO_3)$ have been calculated and compared with the available experimental data. The calculated linear optical properties reveal that there exists a considerable anisotropy thereby favoring an enhanced phase matching conditions necessary for observation of the second harmonic generation (*SHG*) and optical parametric oscillation (*OPO*). It has been found that $LiMoO_3(IO_3)$ posses positive birefringence and negative uniaxial anisotropy. The molybdenyl iodate with $2D-Mo-O$ sheets capped by IO_3^- group is the main source of the *SHG* due to the electronic transition from the lone-pair electrons of oxygen atoms ($O-2p$) to $Mo-4d$ and $I-5p$ states. Moreover, the presence of the alkali metals can give further strength to the *SHG*. We would like to mention that the dipole moments in MoO_6 octahedra and IO_3^- group arranged in a way which strengthens the *SHG*. Our calculated value of the dominant component of the *SHG* agrees well with the experimental value obtained by Chen's group, which is four times larger than that of the well known *KDP* (KH_2PO_4). Also we found that it is equal to one half of the experimental value of the well known $KTiOPO_4$ (*KTP*) single crystals. Further, from the obtained *SHG* values of the dominant components we have calculated the microscopic first hyperpolarizability at static limit and at $\lambda = 1064$ nm.

1. Introduction

The nonlinear optical (*NLO*) materials have been considered as potential candidates due to their numerous applications in nonlinear optics and laser engineering. The borate materials BaB_2O_4, LiB_3O_5, CsB_3O_5, $BaBiBO_4$, $Bi_2ZnB_2O_7$, $CaBiGaB_2O_7$, $Bi_2CaB_2O_7$, $Bi_2SrB_2O_7$ and $YCa_4(BO_3)_3O$ are all well-known *NLO* crystals [1–4] which show excellent properties such as short growth period, large effective nonlinear coefficient, high damage threshold, and good mechanical properties. Searching for novel nonlinear optical materials which can present a relatively new class of functional materials with large and extremely fast nonlinearities compared to traditional *NLO* crystals is very challenging. A development in the research of nonlinear optics of novel inorganic and organic semiconducting materials, has gained great interest for second- and third-order *NLO* applications due to their large optical nonlinearities and their ultrafast, almost purely electronic response [5–16]. These materials offer many possibilities to tailor materials with the desired properties through optimization of the microscopic hyperpolarizabilities (molecular engineering) and the incorporation of molecules in a crystalline lattice (crystal engineering) and polymers. The research on inorganic and organic materials for photonic elements is strongly motivated by the need for the development of high transmission bandwidths and wavelength division multiplexing systems in telecommunication technologies [13–16]. For high speed second-order nonlinear optical applications, such as electro-optics, second-harmonic generation (*SHG*), optical parametric oscillation (*OPO*), and optical rectification, including THz wave generation, a highly asymmetric electronic response of the material to the external electric field is required. It is important to understand the relation between the structure and the main sources of the *NLO* properties. Also it is essential to understand the relation between molecular ordering with noncovalent interactions. This can be obtained from calculating and analyzing

---

[*] Corresponding author. New Technologies – Research Centre, University of West Bohemia, Univerzitni 8, 306 14 Pilsen, Czech Republic.
E-mail address: maalidph@yahoo.co.uk (A.H. Reshak).

http://dx.doi.org/10.1016/j.jallcom.2015.11.076
0925-8388/© 2015 Elsevier B.V. All rights reserved.

the linear optical properties. The calculation of the linear optical properties involve the energy eigenvalues and electron wave-functions. These are natural outputs of the band structure calculations. Therefore, the linear optical properties give deep insight into the electronic structure. For *NLO* crystals, it is very well known that a different orientation of chromophores essentially affects the macroscopic *NLO* properties [17,18]. However, the influence of various noncovalent interactions on the microscopic and macroscopic nonlinearities is not understood yet [17]. Understanding and exploitation of noncovalent interactions in molecular crystals are therefore a starting point of our motivation for this work. It has been reported that the $LiMoO_3(IO_3)$ represents a new structure type and the first structurally characterized molybdenyl iodate with $2D-Mo-O$ sheets capped by IO_3^- group which is the main sources for *SHG* [19,20]. Furthermore, Hu and Mao [20] reported that $LiMoO_3(IO_3)$, $RbMoO_3(IO_3)$ and $CsMoO_3(IO_3)$ have the same chemical formula and their structure contains several distorted MoO_6 and IO_3^- groups but $LiMoO_3(IO_3)$ presented the highest *SHG* among $RbMoO_3(IO_3)$ and $CsMoO_3(IO_3)$. Therefore, to investigated the reason beyond the strong *SHG* of $LiMoO_3(IO_3)$, we have addressed ourselves to investigate the linear optical susceptibilities of $LiMoO_3(IO_3)$ which will bring us important insights to understand the electronic origins of the nonlinear optical susceptibilities and the hyperpolarizability by employing first-principles calculations using the full potential linear augmented plane wave plus local orbitals ($FP-LAPW+lo$) method which has proven to be one of the accurate methods [21–24] for the computation of the electronic structure of solids within density functional theory (*DFT*).

2. Calculation methodology

The current calculations were performed based on the x-ray crystallographic data reported by Chen's group [15]. The geometrical relaxation was achieved within the generalized gradient approximation ($PBE-GGA$) [25] using the full potential linear augmented plane wave ($FP-LAPW+lo$) method as embodied in the *WIEN2k* code [26]. The resulting relaxed geometry was used to calculate the linear and nonlinear optical susceptibilities using $PBE-GGA$ and the recently modified Becke-Johnson potential (*mBJ*) [27]. The crystal structures of $LiMoO_3(IO_3)$ is presented in Fig. 1. The muffin-tin radii (R_{MT}) of the atoms are chosen in such a way that the spheres did not overlap. The value of R_{MT} is taken to be 1.84 a.u. (I), 1.63 a.u. (Li), 1.71 a.u. (Mo) and 1.55 a.u. for O. To achieve the total energy convergence, the basis functions in the interstitial region (*IR*) were expanded up to $R_{MT} \times K_{max} = 7.0$ and inside the atomic spheres for the wave function. The maximum value of $\boldsymbol{l}$ was taken as $\boldsymbol{l}_{max} = 10$, while the charge density is Fourier expanded up to $G_{max} = 12\ (a.u.)^{-1}$. Self-consistency is obtained using 300 $\overline{k}$ points in the irreducible Brillouin zone (*IBZ*). The self-consistent calculations are converged since the total energy of the system is stable within 0.00001 Ry. The linear optical properties are performed within 1500 $\overline{k}$ points in the *IBZ*, while the nonlinear optical properties are performed within 2400 $\overline{k}$ points in the *IBZ*.

3. Results and discussion

3.1. Linear optical properties and birefringence

Based on the electronic band structure calculations the imaginary and real parts of the frequency dependent optical dielectric functions were calculated. The calculations of the optical dielectric functions involve the energy eigen-values and electron wave-functions. These are natural outputs of band structure calculations, thus the calculated dielectric functions give deep insight to understand the electronic structure. The optical tensors are determined by inter-band transitions between the valence bands (*VB*) and the conduction bands (*CB*). According to the dipolar selection rule only transitions changing the angular momentum quantum number *l* by unity ($\Delta = \pm 1$) are allowed. We have calculated $\varepsilon_2^{xx}(\omega)$, $\varepsilon_2^{yy}(\omega)$ and $\varepsilon_2^{zz}(\omega)$, which are the imaginary part of the dielectric function. These completely describe the linear optical response. These tensor components can be obtained from the momentum matrix elements between the occupied and unoccupied wave-functions, giving rise to the selection rules as shown in Fig. 2(a) and (b). To completely identify the origin of the observed optical spectral structures in $\varepsilon_2^{xx}(\omega)$, $\varepsilon_2^{yy}(\omega)$ and $\varepsilon_2^{zz}(\omega)$ we need to carefully look at the magnitude of the optical matrix elements. The observed structures would correspond to those transitions that have large optical matrix elements. To simplify this we have indicated the allowed optical transitions ($\Delta = \pm 1$) between the *VB* and *CB* using our calculated electronic band structure (Fig. 2(b)). The allowed optical transitions occurs between O-2s/2p, Mo-4p, I-5s/5p/4d, Li-2s and Mo-4p/4d, I-5s/4d, Li-2s states to form the first optical spectral structure. It is interesting to mention that the width of the first optical spectral structure is essentially determined by the width of the highest occupied *VB*. The second optical spectral structure corresponds to transition between Mo-5s/4p/4d, O-2p, I-5s/5p/4d, Li-2s and Mo-4p/4d, O-2s/2p, Li-2s, I-5s/5p/4d states. The broadening is chosen to be 0.1 eV which is typical of the experimental accuracy and it is traditional for oxide compounds. Since the *mBJ* succeeds by large amount in bringing the calculated energy gap closer to the experimental one (see Fig. S1 – supplementary materials), all discussions are for *mBJ*. The fundamental optical absorption edge for $\varepsilon_2^{xx}(\omega)$, $\varepsilon_2^{yy}(\omega)$ and $\varepsilon_2^{zz}(\omega)$ are located at 2.73 eV, the value of the fundamental optical gap, which confirms the occurrence of the accurate optical transitions between the top of *VB* and bottom of *CB* as shown in Fig. 2(b). Following Fig. 2(a) we can see there exists a considerable anisotropy between the optical tensor components in the [100], [010] and [001] polarization directions. This anisotropy favors an enhanced phase matching conditions necessary for observation of *SHG* and *OPO*. It has been noticed

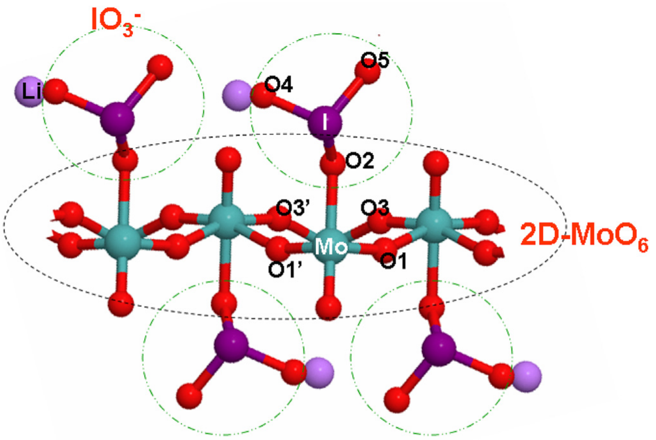

Fig. 1. Crystal structure of $LiMoO_3(IO_3)$. It is clear that the Mo atom occupied a distorted octahedron with short Mo–O6 bond, here O6 is not bound to any other atoms. Four Mo–O–Mo bonds through O1, O1′, O3 and O3′ and one Mo–O–I link by O2. It has been reported that the $LiMoO_3(IO_3)$ represents a new structure type and the first structurally characterized molybdenyl iodate with 2D-Mo-O sheets capped by IO_3^- group.